Proc. Natl. Acad. Sci. USA
Vol. 93, pp. 3335–3340, April 1996
Biophysics

Oxidation states of the manganese cluster during the flash-induced S-state cycle of the photosynthetic oxygen-evolving complex

THEO A. ROELOFS†‡§¶, WENCHUAN LIANG†‡‖, MATTHEW J. LATIMER†‡, ROEHL M. CINCO†‡, ANNETTE ROMPEL†‡, JOY C. ANDREWS†‡, KENNETH SAUER†‡§, VITTAL K. YACHANDRA†§, AND MELVIN P. KLEIN†§

†Structural Biology Division, Lawrence Berkeley National Laboratory, and ‡Department of Chemistry, University of California, Berkeley, CA 94720

Communicated by Sung-Hou Kim, University of California, Berkeley, CA, December 15, 1995 (received for review August 18, 1995)

ABSTRACT **The Mn K-edge x-ray absorption spectra for the pure S states of the tetranuclear Mn cluster of the oxygen-evolving complex of photosystem II during flash-induced S-state cycling have been determined. The relative S-state populations in samples given 0, 1, 2, 3, 4, or 5 flashes were determined from fitting the flash-induced electron paramagnetic resonance (EPR) multiline signal oscillation pattern to the Kok model. The edge spectra of samples given 0, 1, 2, or 3 flashes were combined with EPR information to calculate the pure S-state edge spectra. The edge positions (defined as the zero-crossing of the second derivatives) are 6550.1, 6551.7, 6553.5, and 6553.8 eV for S_0, S_1, S_2, and S_3, respectively. In addition to the shift in edge position, the $S_0 \rightarrow S_1$ and $S_1 \rightarrow S_2$ transitions are accompanied by characteristic changes in the shape of the edge, both indicative of Mn oxidation. The edge position shifts very little (0.3 eV) for the $S_2 \rightarrow S_3$ transition, and the edge shape shows only subtle changes. We conclude that probably no direct Mn oxidation is involved in this transition. The proposed Mn oxidation state assignments are as follows: S_0 (II, III, IV, IV) or (III, III, III, IV), S_1 (III, III, IV, IV), S_2 (III, IV, IV, IV), S_3 (III, IV, IV, IV).**

Photosynthetic oxygen evolution occurs at a specialized site of photosystem II (PSII), the oxygen-evolving complex (OEC) (reviewed in refs. 1 and 2). To couple the single-electron photochemistry of the PSII reaction center to the four-electron oxidation of two water molecules to molecular oxygen, the OEC cycles through five intermediate states, denoted S_i, where the index i indicates the number of positive charges accumulated at the OEC and runs from 0 to 4. The S_1 state is the dark stable state. The S_4 state is thought to decay spontaneously back to the S_0 state, releasing a dioxygen molecule. The OEC contains a tetranuclear manganese cluster that has been implicated as the catalytic site for water oxidation. The mode of charge accumulation during S-state cycling is of particular interest and can be studied by electron paramagnetic resonance (EPR) and x-ray absorption spectroscopy (XAS) (reviewed in ref. 3).

The S_2 state of the OEC exhibits a broad EPR signal, centered near $g = 2$, that shows at least 19 partially resolved Mn hyperfine lines (4, 5). This multiline signal (MLS) is indicative of a mixed valence Mn cluster of possibly four exchange-coupled Mn atoms and can be used as a quantitative marker for the S_2 population. The Mn K-edge x-ray absorption spectrum, in particular the edge region (x-ray absorption near edge structure, XANES), can be used to monitor the oxidation state of the Mn cluster. Upon advance of the OEC from S_1 to S_2, the Mn K-edge of PSII shifts to higher energy by 1–2 eV, which has been interpreted as evidence for direct Mn oxidation (6–8). Additional results were obtained on S_0- and S_3-like states, referred to as S_0^* and S_3^*, respectively, that were populated by low-temperature continuous illumination of chemically treated samples. In the S_3^* state, the OEC was shown to have the same Mn K-edge position as in S_2, suggesting the absence of direct Mn oxidation during the $S_2 \rightarrow S_3$ transition (9). During the $S_0 \rightarrow S_1$ transition, Mn appears to be oxidized, because the inflection point energy of the S_1 state is ≈2 eV higher than that in the S_0^* state (10).

A promising approach to study the Mn oxidation states in the native S states is to step samples through the S-state cycle by application of saturating single-turnover flashes and characterize these samples by XANES spectroscopy. Significant improvements in detection systems have made XAS experiments on samples in a single-flash saturable concentration regime possible. The first Mn XANES experiments on flash-induced S states have recently been reported (11–13). The occurrence of similar shifts in the edge position upon the first and second flash led those authors to conclude that direct Mn oxidation takes place during both the $S_1 \rightarrow S_2$ and the $S_2 \rightarrow S_3$ transitions (11). However, in those XANES studies no independent information was available on the actual S-state distributions in the XAS samples used.

Because of the apparent discrepancy between the results of Ono *et al.* (11) and our previous studies (9, 10), we decided to combine XANES experiments on flash-induced S-states with a detailed EPR characterization of the flash-induced S-state advance in the same samples. We have monitored the S_2 population by measuring its EPR MLS amplitude and have fit the damped oscillation pattern with the Kok model, using misses and double hits as the only variables (14, 15). This model allows for the calculation of flash-induced S-state distributions, which are crucial for accurate extraction of the edge spectra of the pure S states from the experimentally acquired flash-induced spectra. The resulting spectra show an edge shift of ≈1.7 eV to higher energy during both the $S_0 \rightarrow S_1$ and the $S_1 \rightarrow S_2$ transitions, accompanied by characteristic changes in the shape of the edges. Both these results are indicative of direct Mn oxidation. In contrast, during the $S_2 \rightarrow S_3$ transition, the position of the edge shifts very little (0.3 eV) and the shape exhibits only subtle changes, suggestive of the absence of a direct Mn-oxidation step. In addition, the inflection point energy and edge shape of the S_0-state spectrum might indicate the presence of Mn(II). These results are consistent with the earlier studies by Guiles *et al.* (9, 10) and are at variance with

The publication costs of this article were defrayed in part by page charge payment. This article must therefore be hereby marked "*advertisement*" in accordance with 18 U.S.C. §1734 solely to indicate this fact.

Abbreviations: EPR, electron paramagnetic resonance; FWHM, full-width at half-maximum; IPE, inflection-point energy; MLS, multiline signal; OEC, oxygen-evolving complex; PSII, photosystem II; XANES, x-ray absorption near edge structure; XAS, x-ray absorption spectroscopy.

§To whom reprint requests should be sent at the † address.
¶Present address: Department of Physics, Free University Berlin, Arnimallee 14, D-14195 Berlin, Germany.
‖Present address: Department of Biochemistry, Beckman Center, Stanford University School of Medicine, Stanford, CA 94305.

those reported by Ono *et al.* (11), especially with regard to the $S_2 \rightarrow S_3$ transition.

MATERIALS AND METHODS

PSII Sample Preparation and Synchronization. PSII-enriched membranes were isolated from spinach according to a modified BBY procedure (described in ref. 8), with the Triton X-100 incubation time reduced to 1 min. These preparations had a chlorophyll (Chl) a/b ratio of 2.0 ± 0.1 and an oxygen evolution rate of 400–550 μmol of O_2/(h·mg of Chl). The PSII membranes were suspended in buffer [15 mM NaCl/5 mM $MgCl_2$/5 mM $CaCl_2$/50 mM Mes/NaOH, pH 6.5/50% (vol/vol) glycerol] to a final Chl concentration of 4–5 mg/ml. Phenyl-*p*-benzoquinone (Eastman Kodak) was added to the samples to a final concentration of 500 μM. The sample suspension was then filled into sample cells (Lucite frames with inner dimensions 18 × 2.5 × 0.8 mm, backed with mylar tape) and subsequently dark-adapted for at least 1 h at 4°C before being frozen in liquid nitrogen. The amplitudes of the tyrosine Y_D^+ EPR signals of these samples were then measured. The sample holders are designed such that the EPR and x-ray experiments are performed on the same samples.

The samples were next raised to room temperature (22–24°C, in the dark for at least 20 min) and the following flash procedure was applied. The light flashes were produced by a Xe flash lamp system (CHH 174; ILC Inc.), which produces white light flashes of 14 μs full-width at half-maximum (FWHM). To maintain maximal synchronization of the PSII centers upon flash illumination, fast recombination reactions between the S_2 and S_3 states and the reduced form of the redox-active tyrosine residue Y_D [occurring in those centers initially residing in the S_1-Y_D state (16)] must be suppressed. This was achieved by application of two preflashes, followed by a 60-min dark adaptation period at room temperature (modified from ref. 17). This procedure synchronizes almost all PSII centers into the S_1-Y_D^+ state. Each sample was next given 0, 1, 2, 3, 4, or 5 flashes, with 1.5 s intervals between individual flashes. After the last flash, the samples were frozen within 1–2 s by immersion in liquid nitrogen. The EPR spectra (both the Y_D^+ signal and the MLS) were recorded and the samples were stored at 77 K for further use in the XANES experiments (within 10 days).

EPR Spectroscopy. EPR spectra were recorded with a Varian E-109 X-band spectrometer equipped with an E-102 microwave bridge. Sample temperature was maintained by an Air Products helium flow cryostat. Spectrometer conditions were as follows: For the Y_D^+ signal, sample temperature, 18 K; microwave power, 0.5 μW at 9.21 GHz; field modulation amplitude, 3.2 mT at 100 kHz; the Y_D^+ signal was quantitated by the peak-to-trough amplitude. For the MLS, sample temperature, 8 K; microwave power, 11 mW at 9.21 GHz; field modulation amplitude, 3.2 mT at 100 kHz; typically 2–4 scans were averaged; the MLS was quantitated by averaging the peak-to-trough amplitudes of three low-field and three high-field lines. To check for possible radiation damage during the XANES experiments, the EPR spectra of the samples were also measured after exposure to x-rays. Typically, the MLS amplitude was ≥80%, relative to the amplitude before x-ray exposure. No free Mn^{2+} EPR signal was detected in any of these samples, indicating that no significant sample degradation occurred during the course of the XANES data collection (typically 6–8 h).

XANES Spectroscopy. Most of the Mn x-ray absorption K-edge spectra were collected at the wiggler beamline 7–3 at the Stanford Synchrotron Radiation Laboratory during dedicated operation of SPEAR (40–100 mA at 3.0 GeV); some spectra were collected at the bending magnet beamline X9B at the National Synchrotron Light Source (100–250 mA at 2.5 GeV). The x-ray beam was used unfocused, with a Si <220> double-crystal monochromator, detuned to 50% total flux to attenuate harmonics. Typical beam size was 11 × 1 mm. The sample was maintained at 10 ± 1 K in a gaseous helium atmosphere by a helium flow cryostat (CF1208A Oxford Instruments). The Mn x-ray absorption spectra were recorded as fluorescence excitation spectra (18), using a 13-element energy-resolving Ge solid-state detector [Canberra Instruments (19)]. Typical Mn fluorescence count rates for the central detector channel were 120 counts per s at 6500 eV (below the Mn K-edge) and 260 counts per s at 6600 eV (above the edge). Spectra were recorded from 6520 to 6580 eV at 0.2 eV intervals with a dwell time of 3 s per point. Energy calibration and resolution were monitored by simultaneous measurement of the absorption spectrum of $KMnO_4$, using its narrow pre-edge line at 6543.3 eV (FWHM ≤ 1.7 eV).

Typically 16–20 scans were averaged for each sample. A linear background, fit to the signal from 6520 to 6535 eV (i.e., before the pre-edge) was subtracted, and the spectra were normalized at the energy of maximal absorption. The position of the main edge was chosen to be defined by its first inflection-point energy (IPE), which was determined from the zero-crossing of the second derivative of the spectrum. Analytical differentiation of a third-order polynomial fit to the data over an interval of 3.0 eV on each side of a data point produced the derivative spectra. The estimated error in the IPE is ±0.1 eV for individual samples. Defining the edge position as the zero-crossing energy of the second derivative of the edge rather than as the half-height energy has the advantage of being relatively insensitive to curved background contributions to the edge spectrum, which are substantial for such dilute samples. For this reason, using the IPE is our method of choice for characterizing the edge position. The second derivative signal was also used to characterize the shape of the edge spectrum as described (20, 21).

$Mn(III)_4(\mu_3\text{-}O)_2(AcO)_7(2,2'\text{-bipyridine})_2(ClO_4)$ (22) and $Mn(IV)_4(\mu_2\text{-}O)_6(1,4,7\text{-triazacyclononane})_3(ClO_4)_4$ (23) were generously provided by our collaborators George Christou and Karl Wieghardt and their research group members, respectively.

RESULTS AND DISCUSSION

S-State Distributions. To extract accurate edge spectra of the pure S states from the measured flash-induced edge spectra, the actual S-state distributions in samples given a particular number, 0–5, of flashes was established by characterizing the flash-induced oscillation pattern of the MLS. This oscillation pattern is shown in Fig. 1. The data shown are from one set of experiments, which consisted of 3–5 samples per flash number. Two other such sets of experiments consisting of 3–4 samples per flash number were also performed (data not shown). The standard deviation in the average multiline amplitude as a function of flash number from each such set was ≈5%. Samples dark-adapted after the preflash treatment did not exhibit any detectable MLS. The first flash induced the maximal amount of MLS. The second flash led to a reduction in MLS to ≈25% of the maximal value. The MLS nearly disappeared (≈5%) after the third flash. The fourth flash led to a slight recovery in MLS amplitude (≈15%), whereas upon the fifth flash the MLS recovered to ≈50% of the maximal value. Thus, the MLS oscillation pattern exhibits a periodicity of four, with maxima after the first and fifth flash, as expected (15).

Saturation of the PSII turnover by the light flashes was ensured in two ways. First, the MLS amplitude induced by 1 flash was compared with that of an identical sample subjected to a low-temperature continuous illumination (10 min at 190 K) commonly used to generate a maximal amount of the MLS S_2 state (24). These amplitudes were indistinguishable within the accuracy of the MLS amplitude determination. We addi-

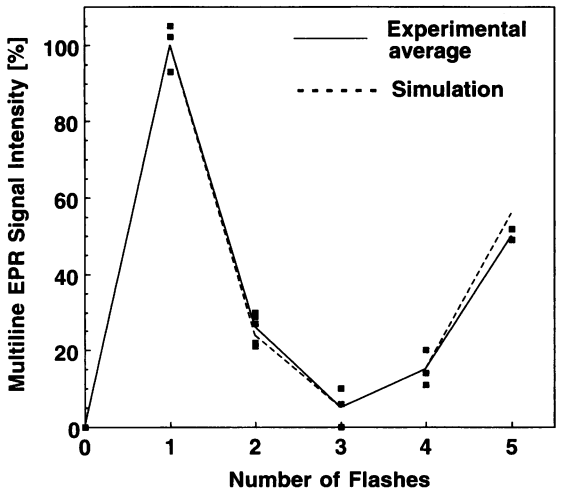

FIG. 1. Flash-induced EPR MLS oscillation pattern of PSII membranes. The MLS amplitudes were normalized to the amplitude after the first flash. Solid line shows the average of 3–5 independent samples per flash number; dashed line is the best fit to the MLS oscillation pattern, using Kok's model with 12% misses and 5% double hits. Two other sets of experiments consisting of 3 or 4 samples per flash number were also performed (data not shown) and their S-state compositions were similarly derived. The standard deviation in the multiline EPR measurements from all the samples is ≈5%.

tionally determined the flash-intensity dependence of the MLS amplitude for a single flash. Using only 60% of the maximal flash intensity, the MLS was 95% of the maximal amplitude. Reducing the energy to 25% resulted in 80% of the maximum MLS. Both observations indicate that the full-intensity flashes were saturating, so that a reasonably small value for the miss parameter can be expected.

Fast recombination reactions between reduced Y_D and the S_2 and S_3 states (see *Materials and Methods*) can be minimized by using a preflash illumination protocol to oxidize Y_D to Y_D^+. The preflash treatment led to an increase in the amplitude of the Y_D^+ signal, typically by 30–50%. The application of 0–5 flashes after the preflash protocol did not lead to a further increase of the Y_D^+ signal, indicating that at that point the recombination between reduced Y_D and the higher S states did not take place to any significant extent. Flash-induced S-state advance can thus be described in terms of only two parameters (misses and double hits), neglecting recombination processes involving reduced Y_D.

Assuming that after the preflash protocol the samples have a 100% S_1 population, the Kok model describes the damped period-four MLS oscillation well (Fig. 1). The best fit (dashed line) was found with 12% misses and 5% double hits.** Using these fit values, the S-state distributions in samples given 0, 1, 2, 3, 4, or 5 flashes were calculated and are given in Table 1. This independent information on the S-state distributions allows us to extract reliably the XANES spectra of the pure S states from the experimentally acquired spectra of flashed samples (see below).

Mn K-Edge Spectroscopy. *Flash-induced changes.* Mn K-edge spectra were measured for three sets of samples. Each set consisted of 2–4 samples given 0–5 flashes; in total a distribution of 7, 8, 12, 8, 6, and 8 samples given 0, 1, 2, 3, 4, and 5 flashes, respectively. The position of the main edge was characterized by its first IPE. In Fig. 2 we show the IPE as a function of the number of flashes applied to the PSII membranes for one such set of samples (3–4 samples per flash number). Samples not given any flash (after the preflash treatment) have a Mn K-edge near 6551.8 eV. The first flash induced a shift of 1.5–2.0 eV to higher energy, shifting the edge to ≈6553.5 eV. Upon the second flash, only a small shift of 0.3 eV to higher energy was observed. Application of the third flash led to a large shift of the edge to lower energy, resulting in an edge position near 6550.5 eV, well below that of a 0-flash sample. The fourth and fifth flashes returned the edge to higher energies.

**In one set we used nanosecond light flashes (frequency-doubled output of a Q-switched Nd-YAG laser, 532 nm, 7 ns FWHM) to step through the S-state cycle; the resulting MLS oscillation was best fit with values for the miss and double-hit parameters of 14% and 0%, respectively.

Table 1. S-state composition (%) of flash-illuminated PSII membranes calculated from the best fit to the MLS oscillation pattern, with 12% misses and 5% double hits

Flash no.	S_0	S_1	S_2	S_3	MLS
0	0	100	0	0	0
1	0	12	83	5	100
2	8	2	20	70	24
3	60	11	4	25	5
4	28	52	12	7	14
5	10	30	46	14	55

Last column reports relative MLS amplitude, normalized to the amplitude after the first flash.

S-state edge spectra. The edge spectrum of a sample subjected to any number of flashes is a superposition of the edge spectra of the four S states, each of these S-state spectra weighted by its population in that particular sample. As described above, application of the Kok model to fit the flash-induced MLS oscillation pattern (Fig. 1) yields an estimate for these relative populations in the individual S-states as a function of the flash number (Table 1). Thus, the pure edge spectra of the four S states can be calculated by inversion of any combination of four equations from Table 1. We used the spectra of samples given 0, 1, 2, or 3 flashes to calculate the edge spectra of the pure states S_0–S_3. The resulting S-state edge spectra are shown in Fig. 3. We tested the accuracy of this procedure by using the appropriate coefficients from Table 1 to reconstruct the edge spectra of a sample given 4 or 5 flashes as a linear combination of the calculated pure S-state spectra. These reconstructed edge spectra agree well with those experimentally observed (25).

The IPE found for the pure S-state spectra are 6550.1, 6551.7, 6553.5, and 6553.8 eV for S_0, S_1, S_2, and S_3, respectively. The standard deviation calculated is 0.2 eV for the S_0-, S_1-, and

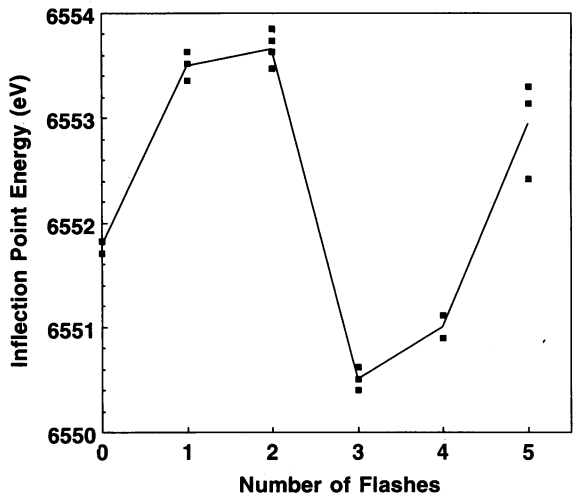

FIG. 2. IPE (in eV) of the Mn K-edge of PSII membranes as a function of the number of applied flashes. Shown are the IPE values of 3 or 4 individual samples per flash number (■) and their averages (—).

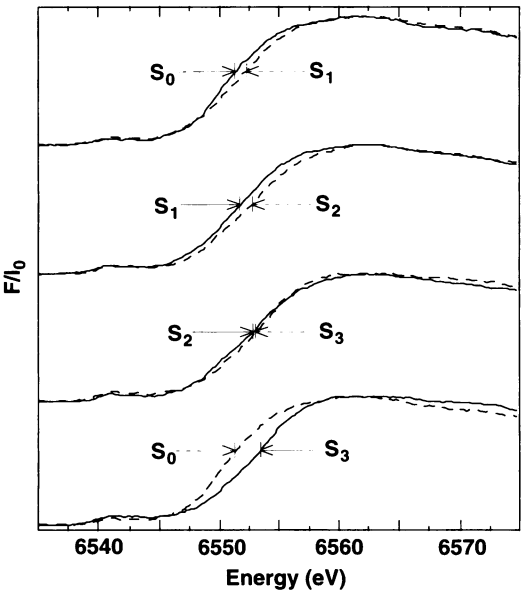

FIG. 3. Normalized Mn K-edge spectra for pure S states of the Mn cluster of PSII, as calculated from the flash-induced edge spectra of samples given 0, 1, 2, or 3 flashes. These are the averages of the S-state spectra extracted from three different sets of samples, each set consisting of 2–4 samples per flash number, in total a distribution of 7, 8, 12, 8, 6, and 8 samples given 0, 1, 2, 3, 4, and 5 flashes, respectively. A linear scatter background was subtracted, and the spectra were normalized at the energy of maximal absorption. To emphasize the changes during the various S-state transitions, the spectra of successive S states are overlaid.

S_2-state spectra and 0.1 eV for the S_3-state spectra. Each of the $S_0 \rightarrow S_1$ and the $S_1 \rightarrow S_2$ transitions is accompanied by a shift of the edge to higher energies by 1.6–1.8 eV, indicating that during those transitions the Mn cluster undergoes oxidation. The $S_2 \rightarrow S_3$ transition, however, leads to a small edge shift of only 0.3 eV, consistent with the absence of a direct Mn-oxidation step. These interpretations are supported by an extensive collection of data on model compounds (3), which indicates that for compounds with similar ligand environments a Mn oxidation is always accompanied by a positive shift in edge position between 1 and 2 eV. On the other hand, compounds with identical oxidation states for Mn, but with different coordination environments, differ in edge position by 0.6 eV at most. This suggests that the observed edge shift during the $S_2 \rightarrow S_3$ transition is more likely caused by a change in the ligand environment of the Mn cluster than by direct Mn oxidation.

The shape of the Mn edge is informative with regard to changes of the oxidation state of the Mn cluster. We previously showed (21) that the spectral region around the inflection point, between 6545 and 6555 eV, reflects predominantly oxidation state changes, whereas the region between 6555 and 6575 eV reflects changes in the coordination environment of the Mn. In Fig. 4 we show the second derivatives of the normalized S-state edge spectra. Several features change reproducibly with S state. During the $S_1 \rightarrow S_2$ transition, a pronounced positive feature appears at 6552 eV, marked with **a**, whereas above 6555 eV the edge remains virtually unchanged. This has also been seen in the edge spectrum of the S_2-state samples populated by continuous illumination at 200 K (25). The shape of the edge in the spectral range between 6545 and 6555 eV (highlighted in the S_3 spectrum in Fig. 4) remains mostly unchanged at the $S_2 \rightarrow S_3$ transition. However, reproducible changes are observed between 6555 and 6575 eV (indicated with **b**, **c**, and **d**). These results suggest that changes occur in the coordination environment of the Mn rather than in the oxidation state of the Mn. The spectrum of the S_0 state

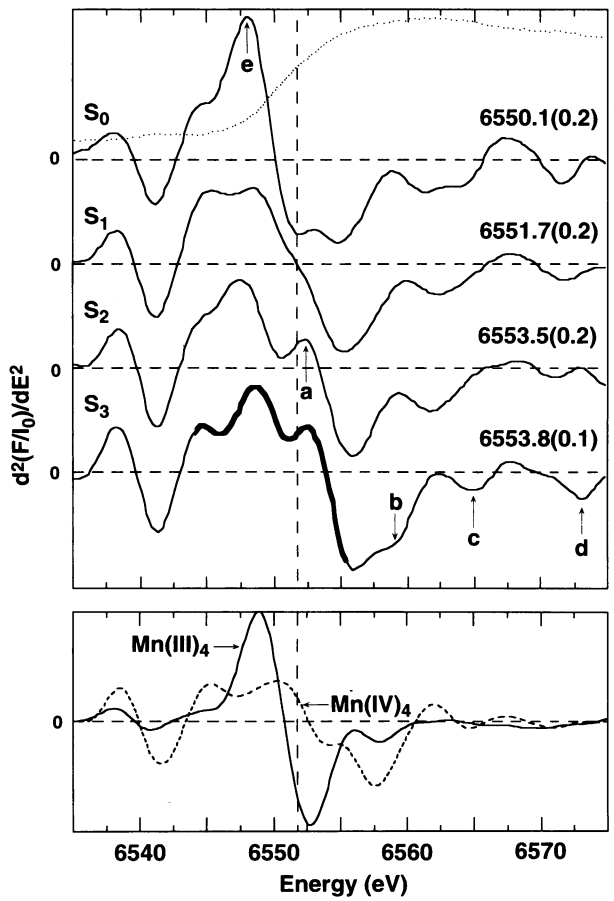

FIG. 4. (*Upper*) Second derivatives of the normalized pure S-state edge spectra shown in Fig. 3 of the Mn cluster of PSII. For clarity, a vertical dashed line has been drawn at the IPE of the S_1 state. The IPE (in eV) for each S state is given at the right and the number in parentheses is the standard deviation. For reference, the spectrum of the S_0 state is plotted as well (dashed line). Features at marked positions **a**–**e** are discussed in the text. (*Lower*) Second derivatives of the normalized Mn K-edge spectra of $Mn(III)_4(\mu_3\text{-}O)_2(AcO)_7$(2,2′-bipyridine)$(ClO_4)$ (solid line) and $Mn(IV)_4(\mu_2\text{-}O)_6$(1,4,7-triazacyclononane)$_3(ClO_4)_4$ (dashed line).

completely lacks feature **a** around 6552 eV. A positive feature around 6548 eV (marked **e**) is present, having a much larger amplitude and a significantly narrower width than that in the S_1 spectrum. This intense and narrow feature is suggestive of the presence of Mn(II) or a greater amount of Mn(III) in the complex (21).

Oxidation State of the Mn Cluster. Based on our analysis of the Mn edge spectra of the flash-induced S states, we propose the following scheme for oxidation states of the Mn cluster during the S-state cycle:

S_0, II, III, IV, IV or III, III, III, IV

S_1, III, III, IV, IV

S_2, III, IV, IV, IV

S_3, III, IV, IV, IV*

In a previous paper (21) we showed that the S_1 state is more likely to consist of Mn_4 (III, III, IV, IV) based on comparison to the Mn K-edge spectra of inorganic model compounds. Upon formation of S_2 one Mn(III) is oxidized to Mn(IV), shifting the edge position to higher energy and giving rise to the EPR MLS (net spin state, 1/2). During the $S_2 \rightarrow S_3$ transition, no direct Mn oxidation occurs for both the position

of the edge and its shape in the 6545 to 6555 eV region change very little. The oxidation equivalent resulting from the reaction center turnover, indicated in the scheme as *, is likely stored in proximity of the Mn cluster, because the MLS disappears (either by coupling of the net spin 1/2 with this positive charge moiety with spin 1/2, or by an alteration in the exchange coupling within the mixed-valence Mn complex). Upon the $S_3 \rightarrow (S_4 \rightarrow)S_0$ transition, the cluster is reset to the most reduced state of the Kok cycle, with the concomitant release of dioxygen. The S_0 state likely contains Mn(II), as judged from the inflection point energy of the K-edge.†† However, based on the shape of the second derivative it is not possible to rule out the oxidation state assignment of III, III, III, and IV. The subsequent transition to the S_1 state involves Mn(II) to Mn(III) oxidation [or Mn(III) to Mn(IV)], resulting in disappearance of the sharp feature **e** in the second derivative of the edge, and a shift in the edge position to higher energy.

The oxidation state assignment for the S_3 state can be further substantiated by comparison with edge spectra of model compounds. If the $S_2 \rightarrow S_3$ transition involved direct Mn oxidation, the S_3 state would consequently be $Mn_4(IV)$. In Fig. 4 (*Lower*), the second derivatives of some typical edge spectra of tetranuclear Mn compounds in oxidation states III and IV are shown. The shape of the edge between 6545 and 6555 eV better supports a model for the Mn cluster containing at least one Mn(III) rather than all Mn(IV).

The Mn oxidation state assignments confirm our previous proposal (3), which was based in part on studies of S_0^* and S_3^* states (9, 10). There is also good agreement with the findings of several other spectroscopic studies on the flash-induced S states. Results from proton–NMR relaxation enhancement experiments (26), from EPR microwave power saturation work (27), and from EPR relaxation studies (17) on the Y_D^+ signal all have been interpreted with the same Mn oxidation state assignment presented here: no change in Mn oxidation state occurring during the $S_2 \rightarrow S_3$ transition and a Mn(II) present in the S_0 state. Results from UV absorption studies have been interpreted preferentially in support of direct Mn oxidation during all three oxidative transitions, although the involvement of ligand oxidation in formation of S_3 was not ruled out completely (28).

The oxidation states we propose differ from existing XANES literature on flash-induced S states by the group of Ono and Kusunoki, in particular concerning the S_0 and S_3 states (11–13). The finding that the first and second flash induced similar shifts in the edge position (defined as half-height energy, HHE) has led those authors to conclude that direct Mn oxidation takes place during both the $S_1 \rightarrow S_2$ and $S_2 \rightarrow S_3$ transitions (11). The different methods for determining the position of an edge (IPE vs. HHE) have been shown probably not to be the major cause of the discrepancies (figure 2 in ref. 13; ref. 25). It is important to note that in the XANES studies by the group of Ono and Kusunoki, no independent information was available on the actual S-state distributions in the samples used. Based on a closer examination of the published data (cf. figure 2 in ref. 13), we suggest that inaccurate accounting for S-state dephasing processes led to underestimation of the edge shift upon the $S_1 \rightarrow S_2$ transition (a shift from 6551.7 to 6552.5 eV), and an overestimation of the edge shift during the $S_2 \rightarrow S_3$ transition [a shift from 6552.5 to 6553.7 eV (11)]. Kusunoki *et al.* (12) also concluded that during the $S_0 \rightarrow S_1$ transition, an oxidation of Mn(III) to Mn(IV) occurs based on the finding that the difference spectra corresponding to each of the oxidative S-state transitions were all similar to one another. This implies that the state of the Mn cluster in the S_0 state would be (III, III, III, IV) rather than (II, III, IV, IV). Without comparisons to spectra of models of known valence, the significance of the difference spectra is difficult to judge. Based on edge shapes, as judged by the second derivatives, we conclude that either Mn(II) → Mn(III) or Mn(III) → Mn(IV) oxidation is possible for the $S_0 \rightarrow S_1$ transition.

Concluding Remark. Based on the analyses of the Mn K-edge spectra for the pure S states, we have presented a model for the oxidation states of the Mn cluster during the flash-induced S-state cycle. To calculate these pure S-state spectra, we combined the spectra of samples given 0, 1, 2, or 3 flashes with independent information on the relative S-state populations in those samples, as extracted from fitting Kok's model to the EPR MLS oscillation pattern. During the $S_2 \rightarrow S_3$ transition, the edge position shifts very little (0.3 eV) and the edge shape shows only subtle changes. Therefore, we conclude that no direct Mn oxidation is involved in this transition. However, at present we cannot rule out completely the possibility that the small shift in edge position and the minor changes in edge structure observed upon the $S_2 \rightarrow S_3$ transition are the net result of two partially compensating effects—namely, direct Mn oxidation and structural rearrangements in the coordination environment of the Mn cluster. Analysis of extended x-ray absorption fine structure data on the flash-induced S_3 state, currently in progress, should provide detailed information on the structure of the Mn cluster in this state.

We thank Dr. H. Frei, Prof. C. B. Harris, and Dr. J. King for providing access to their Nd-YAG laser systems; Dr. B. Chance for the use of his Ge detector; Dr. S. Khalid, Dr. Yang Hai (National Synchrotron Light Source), and Dr. B. Hedman (Stanford Synchrotron Radiation Laboratory) for valuable assistance at the beamlines; Dr. Holger Dau for stimulating discussions; and Gary Olsen for critically reading the manuscript. We are grateful to our collaborators Drs. W. H. Armstrong, G. Christou, J.-J. Girerd, D. Hodgson, K. Wieghardt, and their research group members for generously providing the inorganic model compounds. This research was supported by the Director, Office of Basic Energy Sciences, Division of Energy Biosciences of the U.S. Department of Energy (DOE), under Contract DE-AC03-76SF00098 and by a grant from the National Science Foundation (DMB91-04104). Synchrotron radiation facilities were provided by the Stanford Synchrotron Radiation Laboratory and the National Synchrotron Light Source, both supported by DOE. T.A.R. was supported in part by a postdoctoral fellowship from the Netherlands Organization for Scientific Research (N.W.O.), which is gratefully acknowledged.

1. Debus, R. J. (1992) *Biochim. Biophys. Acta* **1102,** 269–352.
2. Rutherford, A. W., Zimmermann, J.-L. & Boussac, A. (1992) in *The Photosystems: Structure, Function and Molecular Biology*, ed. Barber, J. (Elsevier, Amsterdam), pp. 179–229.
3. Sauer, K., Yachandra, V. K., Britt, R. D. & Klein, M. P. (1992) in *Manganese Redox Enzymes*, ed. Pecoraro, V. L. (VCH, New York), pp. 141–175.
4. Dismukes, G. C. & Siderer, Y. (1981) *Proc. Natl. Acad. Sci. USA* **78,** 274–278.
5. Hansson, Ö. & Andréasson, L.-E. (1982) *Biochim. Biophys. Acta* **679,** 261–268.
6. Goodin, D. B., Yachandra, V. K., Britt, R. D., Sauer, K. & Klein, M. P. (1984) *Biochim. Biophys. Acta* **767,** 209–216.
7. Yachandra, V. K., Guiles, R. D., McDermott, A. E., Cole, J. L., Britt, R. D., Dexheimer, S. L., Sauer, K. & Klein, M. P. (1987) *Biochemistry* **26,** 5974–5981.
8. Liang, W., Latimer, M. J., Dau, H., Roelofs, T. A., Yachandra, V. K., Sauer, K. & Klein, M. P. (1994) *Biochemistry* **33,** 4923–4932.
9. Guiles, R. D., Zimmermann, J.-L., McDermott, A. E., Yachandra, V. K., Cole, J. L., Dexheimer, S. L., Britt, R. D., Wieghardt, K., Bossek, U., Sauer, K. & Klein, M. P. (1990) *Biochemistry* **29,** 471–485.

††A $Mn(II, III)_2$ or $Mn(III, IV)_2$ part of the cluster in the S_0 state might be expected to have a net spin state 1/2 and could therefore exhibit an EPR signal with many lines. However, this has never been observed experimentally.

10. Guiles, R. D., Yachandra, V. K., McDermott, A. E., Cole, J. L., Dexheimer, S. L., Britt, R. D., Sauer, K. & Klein, M. P. (1990) *Biochemistry* **29,** 486–496.
11. Ono, T., Noguchi, T., Inoue, Y., Kusunoki, M., Matsushita, T. & Oyanagi, H. (1992) *Science* **258,** 1335–1337.
12. Kusunoki, M., Ono, T., Noguchi, T., Inoue, Y. & Oyanagi, H. (1993) *Photosynth. Res.* **38,** 331–339.
13. Ono, T., Noguchi, T., Inoue, Y., Kusunoki, M., Yamaguchi, H. & Oyanagi, H. (1994) *Biochem. Soc. Trans.* **22,** 331–335.
14. Kok, B., Forbush, B. & McGloin, M. (1970) *Photochem. Photobiol.* **11,** 457–475.
15. Joliot, P. & Kok, B. (1975) in *Bioenergetics of Photosynthesis*, ed. Govindjee (Academic, New York), pp. 387–412.
16. Vass, I. & Styring, S. (1991) *Biochemistry* **30,** 830–839.
17. Evelo, R. G., Styring, S., Rutherford, A. W. & Hoff, A. J. (1989) *Biochim. Biophys. Acta* **973,** 428–442.
18. Jaklevic, J., Kirby, J. A., Klein, M. P., Robertson, A. S., Brown, G. S. & Eisenberger, P. (1977) *Solid State Commun.* **23,** 679–682.
19. Cramer, S. P., Tench, O., Yocum, M. & George, G. N. (1988) *Nucl. Instrum. Methods A* **266,** 586–591.
20. Conradson, S. D., Burgess, B. K., Newton, W. E., Hodgson, K. O., McDonald, J. W., Rubinson, J. F., Gheller, S. F., Mortenson, L. E., Adams, M. W. W., Mascharak, P. K., Armstrong, W. A. & Holm, R. H. (1985) *J. Am. Chem. Soc.* **107,** 7935–7940.
21. Yachandra, V. K., DeRose, V. J., Latimer, M. J., Mukerji, I., Sauer, K. & Klein, M. P. (1993) *Science* **260,** 675–679.
22. Vincent, J. B., Christmas, C., Huffman, J. C., Christou, G., Chang, H.-R. & Hendrickson, D. N. (1987) *J. Chem. Soc. Chem. Commun.*, pp. 236–238.
23. Wieghardt, K., Bossek, U. & Gebert, W. (1983) *Angew. Chem. Int. Ed. Engl.* **22,** 328–329.
24. Brudvig, G. W., Casey, J. L. & Sauer, K. (1983) *Biochim. Biophys. Acta* **723,** 366–371.
25. Liang, W. (1994) Ph.D. thesis (Lawrence Berkeley Laboratory and Univ. of California, Berkeley).
26. Sharp, R. R. (1992) in *Manganese Redox Enzymes*, ed. Pecoraro, V. L. (VCH, New York), pp. 177–196.
27. Styring, S. A. & Rutherford, A. W. (1988) *Biochemistry* **27,** 4915–4923.
28. Dekker, J. P. (1992) in *Manganese Redox Enzymes*, ed. Pecoraro, V. L. (VCH, New York), pp. 85–103.